



University  
of Glasgow

Gallego-Sala, A. V. et al. (2018) Latitudinal limits to the predicted increase of the peatland carbon sink with warming. *Nature Climate Change*, 8(10), pp. 907-913.

There may be differences between this version and the published version. You are advised to consult the publisher's version if you wish to cite from it.

<http://eprints.gla.ac.uk/168775/>

Deposited on: 14 September 2018

Enlighten – Research publications by members of the University of Glasgow\_  
<http://eprints.gla.ac.uk>

# Latitudinal limits to the predicted increase of the peatland carbon sink with warming

Angela V. Gallego-Sala<sup>1\*</sup>, Dan J. Charman<sup>1\*</sup>, Simon Brewer<sup>2</sup>, Susan E. Page<sup>3</sup>, I. Colin Prentice<sup>4</sup>, Pierre Friedlingstein<sup>5</sup>, Steve Moreton<sup>6</sup>, Matthew J. Amesbury<sup>1</sup>, David W. Beilman<sup>7</sup>, Svante Björck<sup>8</sup>, Tatiana Blyakharchuk<sup>9</sup>, Christopher Bochicchio<sup>10</sup>, Robert K. Booth<sup>10</sup>, Joan Bunbury<sup>11</sup>, Philip Camill<sup>12</sup>, Donna Carless<sup>1</sup>, Rodney A. Chimner<sup>13</sup>, Michael Clifford<sup>14</sup>, Elizabeth Cressey<sup>1</sup>, Colin Courtney-Mustaphi<sup>15,16</sup>, François De Vleeschouwer<sup>17</sup>, Rixt de Jong<sup>8</sup>, Barbara Fialkiewicz-Koziel<sup>18</sup>, Sarah A. Finkelstein<sup>19</sup>, Michelle Garneau<sup>20</sup>, Esther Githumbi<sup>15</sup>, John Hribljan<sup>13</sup>, James Holmquist<sup>21</sup>, Paul D. M. Hughes<sup>22</sup>, Chris Jones<sup>23</sup>, Miriam C. Jones<sup>24</sup>, Edgar Karofeld<sup>25</sup>, Eric S. Klein<sup>26</sup>, Ulla Kokfelt<sup>8</sup>, Atte Korhola<sup>27</sup>, Terri Lacourse<sup>28</sup>, Gael Le Roux<sup>17</sup>, Mariusz Lamentowicz<sup>18,29</sup>, David Large<sup>30</sup>, Martin Lavoie<sup>31</sup>, Julie Loisel<sup>32</sup>, Helen Mackay<sup>33</sup>, Glen M. MacDonald<sup>21</sup>, Markku Makila<sup>34</sup>, Gabriel Magnan<sup>20</sup>, Robert Marchant<sup>15</sup>, Katarzyna Marcisz<sup>18,29,35</sup>, Antonio Martínez Cortizas<sup>36</sup>, Charly Massa<sup>7</sup>, Paul Mathijssen<sup>27</sup>, Dmitri Mauquoy<sup>37</sup>, Timothy Mighall<sup>37</sup>, Fraser J.G. Mitchell<sup>38</sup>, Patrick Moss<sup>39</sup>, Jonathan Nichols<sup>40</sup>, Pirta O. Oksanen<sup>41</sup>, Lisa Orme<sup>1,42</sup>, Maara S. Packalen<sup>43</sup>, Stephen Robinson<sup>44</sup>, Thomas P. Roland<sup>1</sup>, Nicole K. Sanderson<sup>1</sup>, A. Britta K. Sannel<sup>45</sup>, Noemí Silva-Sánchez<sup>36</sup>, Natascha Steinberg<sup>1</sup>, Graeme T. Swindles<sup>46</sup>, T. Edward Turner<sup>46,47</sup>, Joanna Uglow<sup>1</sup>, Minna Väliranta<sup>27</sup>, Simon van Bellen<sup>20</sup>, Marjolein van der Linden<sup>48</sup>, Bas van Geel<sup>49</sup>, Guoping Wang<sup>50</sup>, Zicheng Yu<sup>10,51</sup>, Joana Zaragoza-Castells<sup>1</sup>, Yan Zhao<sup>52</sup>

\*Authors for correspondence

<sup>1</sup>Geography Department, Amory Building, Rennes Drive, University of Exeter, Exeter, EX4 4RJ, United Kingdom

<sup>2</sup>Department of Geography, University of Utah, Salt Lake City, UT, USA

<sup>3</sup>School of Geography, Geology and the Environment, University of Leicester, Leicester, UK

<sup>4</sup>AXA Chair of Biosphere and Climate Impacts, Department of Life Sciences, Imperial College London, Silwood Park, Ascot, UK

<sup>5</sup>College of Engineering, Maths and Physics, University of Exeter, Exeter, UK

<sup>6</sup>NERC Radiocarbon Facility, East Kilbride, UK

<sup>7</sup>Department of Geography, University of Hawaii at Manoa, Honolulu, HI, USA

<sup>8</sup>Department of Geology, Lund University, Lund, Sweden

<sup>9</sup>Institute for Monitoring Climatic & Ecological Systems, Siberian branch of the Russian Academy of Science (IMCES SB RAS), Tomsk, Russia

<sup>10</sup>Department of Earth and Environmental Science, Lehigh University, Bethlehem, PA, USA

<sup>11</sup>Department of Geography and Earth Science, University of Wisconsin-La Crosse, La Crosse, WI, US

<sup>12</sup>Environmental Studies Program and Earth and Oceanographic Science Department, Bowdoin College, Brunswick, ME, USA

<sup>13</sup>School of Forest Research and Environmental Sciences, Michigan Technical University, Houghton, MI, USA

<sup>14</sup>DRI, Division of Earth and Ecosystem Science, Las Vegas, NV, USA

<sup>15</sup>Environment Department, University of York, York, UK

<sup>16</sup>Department of Archaeology and Ancient History, Uppsala Universitet, Uppsala, Sweden

<sup>17</sup>EcoLab, Université de Toulouse, CNRS, INPT, UPS, Castanet Tolosan, France

<sup>18</sup>Department of Biogeography & Palaeoecology, Adam Mickiewicz University, Poznań, Poland

<sup>19</sup>Department of Earth Sciences, University of Toronto, Toronto, Canada

<sup>20</sup>GEOTOP, Université du Québec à Montréal, Canada

<sup>21</sup>Institute of Environment & Sustainability, University of California Los Angeles, Los Angeles, CA, USA

<sup>22</sup>Geography and Environment, University of Southampton, Southampton, UK

<sup>23</sup>MET Office, Hadley Centre, Exeter, UK

<sup>24</sup>USGS, Reston, Virginia, VA, USA

<sup>25</sup>Institute of Ecology & Earth Sciences, University of Tartu, Tartu, Estonia

<sup>26</sup>Department of Geological Sciences, University of Alaska Anchorage, Anchorage, AK, USA

<sup>27</sup>ECRU, University of Helsinki, Helsinki, Finland

<sup>28</sup>Department of Biology and Centre for Forest Biology, University of Victoria, Victoria, Canada

<sup>29</sup>Laboratory of Wetland Ecology & Monitoring, Adam Mickiewicz University, Poznań, Poland

<sup>30</sup>Department Of Chemical and Environmental Engineering, University of Nottingham, Nottingham, UK

<sup>31</sup>Département de Géographie & Centre d'Études Nordiques, Université Laval, Québec City, Canada

<sup>32</sup>Department of Geography, Texas A&M University, College Station, TX, USA

<sup>33</sup>School of Geography, Politics and Sociology, Newcastle University, Newcastle, UK

<sup>34</sup>Geological Survey of Finland, Espoo, Finland

<sup>35</sup>Institute of Plant Sciences & Oeschger Centre for Climate Change Research, University of Bern, Bern, Switzerland

<sup>36</sup>Departamento de Edafología e Química Agrícola, Universidade de Santiago de Compostela, Spain

<sup>37</sup>Geosciences, University of Aberdeen, Aberdeen, UK

<sup>38</sup>School of Natural Sciences, Trinity College Dublin, Dublin, Ireland

<sup>39</sup>School of Earth and Environmental Sciences, The University of Queensland, Brisbane, Australia

<sup>40</sup>Lamont-Doherty Earth Observatory, Columbia University, Palisades, NY, USA

<sup>41</sup>Previously at the Arctic Centre, University of Lapland, Rovaniemi, Finland

<sup>42</sup>Department of Geology and Geophysics, Norwegian Polar Institute, Tromsø, Norway

<sup>43</sup>Science and Research Branch, Ministry of Natural Resources and Forestry, Sault Ste. Marie, Canada

<sup>44</sup>Champlain College, Dublin, Ireland

<sup>45</sup>Department of Physical Geography, Stockholm University, Stockholm, Sweden

<sup>46</sup>School of Geography, University of Leeds, Leeds, UK

<sup>47</sup>The Forestry Commission, Galloway Forest District, Scotland, UK

<sup>48</sup>BIAx Consult, Zaandam, The Netherlands

<sup>49</sup>IBED, Universiteit van Amsterdam, Amsterdam, The Netherlands

<sup>50</sup>Northeast Institute of Geography & Agroecology, Chinese Academy of Science, Changchun, China

<sup>51</sup>Key Laboratory of Wetland Ecology, Institute for Mire and Peat Research, Northeast Normal University, Changchun, China

<sup>52</sup>Institute of Geographical Science & Natural Resources, Chinese Academy of Science, Beijing, China

Key words: peatlands, carbon cycle, climate change, tropical peat, last millennium.

**The carbon sink potential of peatlands depends on the balance between carbon uptake by plants and microbial decomposition. The rates of both these processes will increase with warming but it remains unclear which will dominate the global peatland response. Here we examine the global relationship between peatland carbon accumulation rates during the last millennium and planetary-scale climate space. A positive relationship is found between carbon accumulation and cumulative photosynthetically active radiation during the growing season for mid- to high-latitude peatlands in both hemispheres. However, this relationship reverses at lower latitudes, suggesting that carbon accumulation is lower under the warmest climate regimes. Projections under RCP2.6 and RCP8.5 scenarios indicate that the present-day global sink will increase slightly until ~2100 AD but decline thereafter. Peatlands will remain a carbon sink in the future, but their response to warming switches from a negative to a positive climate feedback (decreased carbon sink with warming) at the end of the 21st century.**

---

Analysis of peatland carbon accumulation over the last millennium and its association with global-scale climate space indicates an ongoing carbon sink into the future, but with decreasing strength as conditions warm.

---

The carbon cycle and the climate form a feedback loop and coupled carbon cycle climate model simulation results show that this feedback is positive<sup>1</sup>. In simple terms, warming of the Earth's surface results in a larger fraction of the anthropogenically and naturally released CO<sub>2</sub> remaining in the atmosphere, inducing further warming. However, the strength of this feedback is highly uncertain; indeed, it is now one of the largest uncertainties in future climate predictions<sup>2</sup>. The terrestrial carbon cycle feedback is potentially larger in magnitude when compared to the ocean carbon cycle feedback, and it is also the more poorly quantified<sup>1,3</sup>. In coupled climate models, there is still no consensus on the overall sensitivity of the land processes, or whether changes in net primary productivity versus changes in

respiration will dominate the response<sup>1</sup>. Furthermore, most models have so far ignored the potential contribution of peatlands, even though they contain 530-694 Gt C<sup>1,4</sup>; equalling the amount of carbon in the pre-industrial atmosphere. The few models that have taken into account the role of peatlands in the carbon cycle predict a sustained carbon sink (global dynamic vegetation models<sup>5,6</sup>) or a loss of sink potential in the future (soil decomposition model<sup>7</sup>) depending on the climate trajectories and the specific model<sup>5,6,7</sup>.

Evidence from field manipulation experiments suggests major future carbon losses from increased respiration in peatlands with warming<sup>8</sup>, but these projections do not take into account the potential increased productivity due to increased temperatures and growing season length, especially in mid- to high-latitude peatlands. Additionally, increased loss of carbon due to warming may be limited to the upper layers of peat but it may not affect the buried deeper anoxic layers<sup>9,10</sup>.

Peatlands preserve a stratigraphic record of net carbon accumulation, the net outcome of both respiration and plant production, and these records can be used to examine the behaviour of the peatland sink over time. This has been done successfully since the last deglaciation (11,700 years ago to the present) at lower resolution<sup>4,11</sup> and for the last millennium (850-1850 AD) at higher temporal resolution<sup>12</sup>. These studies have focused on high latitude northern peatlands and have shown that in warmer climates increases in plant productivity overcome increases in respiration and that these peatlands will likely become a more efficient sink if soil moisture is maintained<sup>11,12,13</sup>.

Here we use 294 profiles from globally distributed peatlands to build a dataset of global carbon accumulation over the last millennium (850-1850 AD) (Figure 1a). We improve the coverage of northern high latitudes and expand the dataset to low latitudes and southern high latitudes by including over 200 new profiles compared to previous data compilations<sup>12</sup>. There are areas of the world where extensive peatlands exist where data are still lacking (e.g. East Siberia, Congo Basin<sup>14</sup>), but our data provide comprehensive coverage of peatland carbon accumulation records over this time period. The last millennium is chosen as a time span because it is climatically relatively similar to the present day enabling comparisons with modern planetary-scale climate space, it is possible to date this part of the peat profile accurately, and the data density is greatest for this period as almost all existing peatlands contain peat from this time.

## Planetary-scale climate effects on the carbon sink

The profiles are predominantly from low nutrient sites (213 sites, Fig 1b), and the spatial patterns of the distribution show that oceanic peatlands tend to be characterised by low nutrients (bogs) while there are continental areas (e.g. central Asia, North America, Arctic Eurasia) where there are extensive higher nutrient peatlands (fens, including poor fens). Mean carbon accumulation rates for the last millennium vary between 3 and 80 g C m<sup>-2</sup> yr<sup>-1</sup> (see Methods, and Figure 1c).

Photosynthetically active radiation summed over the growing season (PAR<sub>0</sub>) is the best explanatory variable of all of the bioclimatic variables that were statistically fitted to carbon accumulation (Figure 2a), in agreement with a previous study of northern peatlands<sup>12</sup>. Carbon accumulation increases almost linearly with increasing PAR<sub>0</sub> up to PAR<sub>0</sub> values of around 8000 mol phot m<sup>-2</sup>, which correspond to peatland sites in the mid-latitudes, including those from the Southern Hemisphere. The positive relationship for PAR<sub>0</sub> is spatially explicit at these mid- to high latitudes, with temperate sites accumulating more carbon than boreal or arctic areas (Figure 1c). The positive relationship peaks at values of PAR<sub>0</sub> ~ 8000 mol phot m<sup>-2</sup> (8000 mol phot m<sup>-2</sup> for bogs and 10,000 mol phot m<sup>-2</sup> for fens), representing sites from mid latitudes, and appears to reverse when PAR<sub>0</sub> > 11,000 mol phot m<sup>-2</sup>, values which represent the tropical sites (Figure 2b). The growing season length at mid latitude locations is at or very close to 365 days a year, so further warming no longer extends the length of the growing season at these sites. The relationship is similar but weaker for growing degree days (GDD<sub>0</sub>, Figure 2c) and growing season length (GSL, Figure SI1c), suggesting that increased accumulation is primarily driven by growing season length, and partly by light availability.

For the lower latitude peatlands, we suggest that the higher temperatures drive increased microbial activity and decomposition rates in the peat and surface litter, but this is not fully compensated by increases in plant productivity (Figure SI4), leading to reduced carbon accumulation rates compared to higher latitude peatlands. It has been shown that plant productivity does not increase with temperature after accounting for the increased length of the growing season<sup>15</sup>. This has important implications in terms of the future carbon sink. Our results suggest that under a future warmer climate, the increase in net primary productivity, due to longer and warmer growing seasons, results in more carbon accumulation only at mid- to high-latitudes. Conversely, increased respiration dominates the response of peatlands to

warming at lower latitudes, even if this warming is predicted to be less compared to the more amplified warming at high latitudes. Thus, the carbon sink of low latitude peatlands will decrease with warmer temperatures, although uncertainty in the carbon accumulation trend for low latitudes is higher, due to the more limited extent of data for these areas. Furthermore, the greater predictive power of PAR0 suggests that light availability is a critical factor in driving the increase in net primary productivity at higher latitudes, in agreement with previous theoretical analysis of plant photosynthesis<sup>16</sup>. Cloud cover and PAR0 remain highly uncertain in future climate projections, and this needs to be considered in estimates of the precise effect of future climate change on peatland carbon accumulation rates.

We expected moisture to be an important controlling variable for carbon accumulation. However, the effect of moisture was not detected using a moisture index (Figure 2d) and instead the relationship between moisture index and carbon accumulation indicates that moisture acts as an on-off switch, i.e. there needs to be sufficient moisture to retard decay but increases to very high moisture levels do not promote higher rates of accumulation. A precipitation deficit analysis was also carried out (Figure SI5) to ascertain whether a greater precipitation shortage drives reduced carbon accumulation, but there are no clear patterns emerging using this moisture parameter either. None of the moisture indexes used account for local small-scale hydrological or water chemistry variations. Because our data does not support a moisture control on global-scale variations in vertical peat accumulation, we have not used moisture as a predictor variable in our future estimates of the carbon sink.

## **The present and future of the carbon sink**

We estimated the total present and future global peatland carbon sink strength using both spatially interpolated observations and statistically modelled data (see methods). According to the spatially interpolated observations (Figure 3a) of last millennium carbon accumulation rates, global peatlands represent an average apparent carbon sink of  $142 \pm 7$  Tg C yr<sup>-1</sup> over the last millennium. This is equivalent to a total millennial sink of  $33 \pm 2$  ppm CO<sub>2</sub>, based on a simple conversion from change in carbon pool to atmospheric CO<sub>2</sub> of  $2.123 \text{ GtC} = 1 \text{ ppm}$  and an airborne fraction of 50 % to account for the carbon cycle response to any carbon dioxide released to or captured from the atmosphere<sup>17</sup>. This figure corresponds to the near-natural sink and does not account for anthropogenic impacts such as land use change, drainage or fires, and also excludes the very slow decomposition that continues in the deeper anoxic

layers of peat older than 1000 years.

There are few directly comparable estimates of the total peatland sink, but a simplistic estimate based on a series of assumptions of average peat depth, extent and bulk density suggested a current rate of 96 Tg C yr<sup>-1</sup> for northern peatlands alone<sup>15</sup>. A subsequent estimate suggests a figure of approximately 110 Tg C yr<sup>-1</sup> global peatland net carbon uptake for the last 1000 years<sup>4</sup> (see Figure 5 in ref. 4), with 90 Tg C yr<sup>-1</sup> in northern peatlands. These estimates are based on averages across very large regions. Our spatially explicit modelling suggests a larger overall carbon sink than these earlier estimates and implies that the size of the global peatland carbon sink is substantially larger than previously thought. This is also a larger value than estimates of the average carbon accumulation rates over the entire Holocene (>50 to 96 Tg C yr<sup>-1</sup>)<sup>4,18</sup>, principally because the total area of peatlands is at its greatest in the last millennium when compared with the earlier in the Holocene. In addition, many high latitude peatlands only accumulated small amounts of peat during the early stages (minerotrophic) of their development, often for several millennia after their initiation<sup>19,20</sup>.

None of the above estimates take into account the long-term decay of previously deposited deeper/older peat. Prior estimates<sup>4</sup> (Figure 5 in ref. 4) suggest that this loss is substantial at around 65 Tg C yr<sup>-1</sup>, producing a net carbon balance of around 45 Tg C yr<sup>-1</sup> compared to a net uptake value of 110 Tg C yr<sup>-1</sup> in the same study. For northern peatlands alone, an earlier estimate of the deep carbon loss<sup>4</sup> was approximately less than half of the equivalent later estimate<sup>9</sup> for the same region, c. 48 Tg C yr<sup>-1</sup>. However, all of these estimates are based on modelling using a ‘super-peatland’ approach combining data from across large areas to estimate mean long term peat decay rates and thus are subject to considerable error. Nevertheless, the net carbon balance including the decay of deeper/older peat is likely to be around a third less than our 142±7 Tg C yr<sup>-1</sup> estimate of the apparent global net uptake over the last millennium, assuming a long-term decay rate between 20 and 50 Tg C yr<sup>-1</sup>.

Modelled changes in the future peatland carbon sink under a warmer climate show a slight increase in the global peatland sink compared to the present-day sink until 2100 AD (RCP 2.6 scenario: 147 ± 7 Tg C yr<sup>-1</sup>; RCP 8.5 scenario: 149± 7 Tg C yr<sup>-1</sup>) and a decrease in the sink thereafter (Figure SI3, Table SI3). The results suggest that initially, and approximately for the next century, peatlands will be a small negative feedback to climate change, i.e. the

global peatland carbon sink increases as it gets warmer. However, this negative feedback does not persist in time and the strength of the sink starts to decline again after 2100 AD, although it remains above the 1961-1990 values throughout the next c.300 years (RCP 2.6 scenario:  $146 \pm 7 \text{ Tg C yr}^{-1}$ ; RCP 8.5 scenario:  $145 \pm 7 \text{ Tg C yr}^{-1}$  for the period 2080-2300). Despite large uncertainties in these projections due to uncertainties originating from both the statistical modelling and from the climate model projections, the direction of change and a shift from initially negative to subsequent positive feedback is a plausible and robust result.

An explanation for the mechanism of change in the sink capacity of the global peatland area can be inferred from the spatial distribution of the modelled changes (Figure 4). While the carbon sink at very high latitudes increases in both RCP2.6 and RCP8.5 scenarios continuously to 2300 AD, the lower latitudes experience an ongoing decrease in carbon sequestration over the same period. Simultaneously, peatlands in the mid latitudes gradually move past the optimum level of photosynthesis/respiration into the decline phase (Figure 2a, Figure SI4) where respiratory losses are rising faster than net primary productivity. This is likely to be determined by the poleward migration of the latitudinal line where the growing season length is near 365 days, moderated by changes in cloud cover and thus PAR. The balance between the increasing high latitude sink, and the decreasing low latitude sink changes over time, such that the global sink eventually begins to decrease. This estimate takes into account only the changes in the surface accumulation rates of extant peatlands and other factors will affect the total peatland carbon balance. Deeper peat may also warm and provide a further source of peatland carbon release in peatlands worldwide, but there is still some debate as to how large this effect may be, especially in the transition from permafrost to unfrozen peatlands<sup>21,22</sup>

Conversely, peatlands may expand into new areas that have previously been too cold or too dry for substantial soil carbon accumulation especially in northern high latitudes, where there are large topographically suitable land areas. The magnitude of these potential changes is unknown, but it would offset at least some of the additional loss of carbon from enhanced deep peat decay. Carbon dioxide fertilization is also likely to increase the peatland carbon sink via increases in primary productivity. Furthermore, vegetation changes and specifically more woody vegetation might result in a larger peatland sink, if moisture is maintained<sup>23</sup>. Increases in shrubs and trees have also been shown to increase the pools of phenolic compounds and decrease the losses of peat carbon to the atmosphere due to inhibitory effects



on decay<sup>24</sup>. All of these changes will be compounded by changes in hydrology, which will also affect overall peatland functioning. None of these potential changes have been taken into account in our projections of the future peatland carbon sink. Finally, human impact on the peatland carbon store is still likely to be the most important determinant of global peatland carbon balance over the next century. Ongoing destruction of tropical peatlands is the largest contributor at present and at current rates, the losses from this source outweigh carbon sequestration rates in natural peatlands<sup>25,26</sup>. Whilst our results are reassuring in showing that the natural peatland C sink will likely increase in future, reducing anthropogenic release of peatland carbon is the highest priority in mitigation of peatland impacts on climate change.

## **Corresponding Authors**

Angela Gallego-Sala and Dan Charman

## **Acknowledgements**

The work presented in this article was funded by the Natural Environment Research Council (NERC standard grant number NE/I012915/1) to D.J.C., A.G.S., I.C.P., S.P. and P.F., supported by NERC Radiocarbon Allocation 1681.1012. The work and ideas in this article have also been supported by PAGES funding, as part of C-PEAT. CDJ was supported by the Joint UK DECC/Defra Met Office Hadley Centre Climate Programme (GA01101). This research is also a contribution to the AXA Chair Programme in Biosphere and Climate Impacts and the Imperial College initiative on Grand Challenges in Ecosystems and the Environment. This research was also supported by a grant from the National Science Centre, Poland 2015/17/B/ST10/01656. We wish to thank Dale Vitt, Jukka Alm, Ilka E. Bauer, Nicole Rausch, Veronique Beaulieu-Audy, Louis Tremblay, Steve Pratte, Alex Lamarre, David Anderson and Alex Ireland for contributing data to this compilation. We are also grateful to Steve Frolking for suggestions on different moisture indexes and to Alex Whittle and Fiona Dearden for their work in the Exeter laboratories.

## **Author Contributions**

A.G.S. carried out analysis and interpretation of the data and wrote the first draft of the paper. D.J.C. supervised the project and contributed to experimental design, interpretation of results, and the final draft. S.B. carried out the statistical and spatial analysis of the data and contributed to the design of the final figures. S.M. was responsible for new radiocarbon analyses. Z.Y. provided the peatland map used in the modelling and contributed data and

material. C.J. provided climate and gross primary productivity (GPP) data. L.O. carried out the age-depth models for all cores. All authors contributed either data or material to be analysed in the Geography laboratories at the University of Exeter. All authors contributed to the preparation of the final paper.

## **Additional Information**

The authors declare no competing financial interest.

## **Figure captions**

Figure 1: Distribution of sampling sites in geographical space. Note that a single point may represent more than one site. (a) Locations of sites shown as either high-resolution records (white circles) or low-resolution records (black circles). (b) Distribution of fen (nutrient rich, green circle) and bog (nutrient poor, blue circle) or mixed (yellow circles) study sites. (c) Distribution of the mean annual carbon accumulation rate during the last millennium ( $\text{gC m}^{-2} \text{yr}^{-1}$ ) for all sites. Light yellow represents the lowest range of mean annual C accumulation ( $0\text{--}10 \text{ gC m}^{-2} \text{yr}^{-1}$ ) while dark brown represents the highest range ( $50\text{--}60 \text{ gC m}^{-2} \text{yr}^{-1}$ ). Colours in between these two shades represent intermediate ranges, separated in  $10 \text{ gC m}^{-2} \text{yr}^{-1}$  intervals.

Figure 2: Controls on peat accumulation rate. Mean annual accumulation over the last 1000 years at each site compared to a) cumulative annual photosynthetically active radiation (PAR0) b) latitude (degrees North are represented by positive numbers and degrees South by negative numbers) c) annual growing degree-days above  $0^{\circ}\text{C}$  (GDD0) and d) the ratio of precipitation over equilibrium evapotranspiration (moisture index, MI). Bog and fen sites (see Figure 1a and supplementary Table 1) are shown in blue and green respectively, and separate regressions have been calculated for each site type for PAR0 ( $R^2$  is shown on the graph). The grey line is the overall regression for all peat types. The regression for GDD0 yielded a much lower  $R^2$  (only shown for all peat types). Errors represent uncertainty in carbon accumulation rates stemming from the age depth model errors (95 percentile range).

Figure 3: Spatial analysis of the overall carbon sink. (a) Gridded spatial distribution of the annual carbon sink based on kriging of observations over the last millennium. Values have been kriged over a present-day peatland distribution map<sup>4</sup>. (b) Gridded spatial distribution of the annual carbon sink based on modelling of carbon accumulation for the last millennium calculated using the statistical relationship between the annual carbon sink and PAR0 (c) Difference between (a) and (b), negative values in red mean an overestimation of the sink using the statistically modelled data when compared with the observations, positive values in blue mean an underestimation of the sink by the model. Note: OK = Observation kriging. RK = Regression kriging

Figure 4: Projected anomalies (future – historic) of annual carbon accumulation rates for three time periods: a) 2040–2060 b) 2080–2100, c) 2180–2200 and d) 2280–2300, based on PAR0 derived from climate data outputs from the Hadley Centre climate model. The climate runs chosen reflect the two end-member representative concentration pathways detailed in the IPCC Fifth Assessment Report<sup>31</sup>: 1) RCP2.5 and 2) RCP8.5.

349  
350

## References

- 351 1 Friedlingstein, P., Cox, P., Betts, R., Bopp, L., von Bloh, W., Brovkin, V., Cadule,  
352 P., Doney, S., Eby, M. Fung, I., Bala, G., John, J., Jones, C., Joos, F., Kato, T.,  
353 Kawamiya, M., Knorr, W., Lindsay, K., Matthews, H.D., Raddatz, T., Rayner, P.,  
354 Reick, C., Roeckner, E., Schnitzler, K.-G., Schnur, R., Strassmann, K., Weaver,  
355 A.J., Yoshikawa, C. and Zeng, N. Climate-Carbon cycle feedback analysis: results  
356 from the C<sup>4</sup>MIP Model Intercomparison. *Journal of climate* **19** 3337-3353 (2006).
- 357 2 Gregory, J.M., Jones, C.D., Cadule, P. and Friedlingstein, P. Quantifying Carbon  
358 Cycle Feedbacks. *Journal of Climate* **22** 5232-5250 (2009).
- 359 3 Matthews, H. D., Eby, M., Ewen, T., Friedlingstein, P. and Hawkins, B.J. What  
360 determines the magnitude of carbon cycle-climate feedbacks? *Global*  
361 *Biogeochemical Cycles* **21** 12 (2007).
- 362 4 Yu, Z.C., Loisel, J., Brosseau, D.P., Beilman, D.W., Hunt, S.J. Global peatland  
363 dynamics since the Last Glacial Maximum. *Geophysical Research Letters*, **37**  
364 L13402 (2010)
- 365 5 Spahni, R., Joos, F., Stocker, B.D., Steinacher, M. and Yu, Z.C. Transient  
366 simulations of the carbon and nitrogen dynamics in northern peatlands: from the  
367 Last Glacial Maximum to the 21<sup>st</sup> century. *Climate of the Past* **9** 1287-1308 (2013)
- 368 6 Chaudhary, N., Miller, P. A., and Smith, B.: Modelling Holocene peatland  
369 dynamics with an individual-based dynamic vegetation model, *Biogeosciences*, **14**,  
370 2571-2596 (2017).
- 371 7 Ise, T., Dunn, A.L., Wofsy, S.C. and Moorcroft, P.R. High sensitivity of peat  
372 decomposition to climate change through water-table feedback. *Nature Geoscience*  
373 **1** 763-766 (2008)
- 374 8 Dorrepaal, E., Toet, S., van Logtestijn, R.S.P., Swart, E., van de Weg, M.J.,  
375 Callaghan, T.V. and Aerts, R. Carbon respiration from subsurface peat accelerated  
376 by climate warming in the subarctic. *Nature* **460** 616-619 (2009)
- 377 9 Wilson, R. M., Hopple, A. M., Tfaily, M. M., Sebestyen, S. D., Schadt, C. W.,  
378 Pfeifer-Meister, L., Medvedeff, C., McFarlane, K. J., Kostka, J. E., Kolton, M.,  
379 Kolka, R.K., Kluber, L. A., Keller, J. K., Guilderson, T. P., Griffiths, N. A.,  
380 Chanton, J. P., Bridgham, S. D. and Hanson, P. J. Stability of peatland carbon to  
381 rising temperatures. *Nature Communications* **7** 13723 (2011)

- 10 Blodau, C., Siems, M. and Beer, J. Experimental burial inhibits methanogenesis and anaerobic decomposition in water-saturated peats. *Environmental Science and Technology* **45** 9984-9989 (2011)
- 11 Loisel, J., Yu, Z., Beilman D.W., Camill, P., Alm, J., Amesbury, M.A., Anderson, D., Andersson, S., Bochicchio, C., Barber, K., Belyea, L.R., Bunbury, J., Chambers, F.M. Charman, D.J., De Vleeschouwer, F., Fiałkiewicz-Kozieł, B., Finkelstein, S.A., Galka, M., Garneau, M., Hammarlund, D., Hinchcliffe, W., Holmquist, J., Hughes, P., Jones, M.C., Klein, E.S., Kokfelt, U., Korhola, A., Kuhry, P., Lamarre, A., Lamentowicz, M., Large, D., Lavoie, M., MacDonald, G., Magnan, G., Mäkilä, M. Mallon, G., Mathijssen, P., Mauquoy, D., McCarroll, J., Moore, T.R., Nichols J., O'Reilly, B., Oksanen, P., Packalen, M., Peteet, D., Richard, P.J.H., Robinson, S., Ronkainen, T., Rundgren, M., Britta, A., Sannel, K., Tarnocai, C., Thom, T., Tuittila, E.-S., Turetsky, M., Väliranta, M., van der Linden, M., van Geel, B., van Bellen, S., Vitt, D., Zhao, Y., and Zhou W. A database and synthesis of northern peatland soil properties and Holocene carbon and nitrogen accumulation. *The Holocene* **24** (9) 1028-1042 (2014).
- 12 Charman, D. J., Beilman, D. W., Blaauw, M., Booth, R. K., Brewer, S., Chambers, F. M., Christen, J. A., Gallego-Sala, A. V., Harrison, S.P., Hughes P.D.M., Jackson S.T., Korhola A., Mauquoy D., Mitchell F.J.G., Prentice I.C., van der Linden M., De Vleeschouwer F., Yu Z.C., Alm J., Bauer I.E., Corish Y.M.C., Garneau M., Hohl V., Y. Huang, E. Karofeld, G. Le Roux, J. Loisel, R. Moschen, Nichols J.E., Nieminen T. M., MacDonald G.M., Phadtare N.R., Rausch N., Sillasoo Ü., Swindles G.T., Tuittila E.-S., Ukonmaanaho L., Väliranta M., van Bellen S., van Geel B., Vitt D.H. and Zhao, Y. Climate-related changes in peatland carbon accumulation during the last millennium. *Biogeosciences* **10** 929–944 (2013).
- 13 Yu, Z. Holocene carbon flux histories of the world's peatlands: Global carbon cycle implications. *Holocene* **21** (5) 761-774 (2010).
- 14 Dargie, G.C., Lewis, S. L., Lawson, I.T., Mitchard E.T.A., Page, S.E., Bocko, Y.E., and Ifo S.A. Age, extent and carbon storage of the central Congo Basin peatland complex. *Nature* **542**, 86-90 (2017).
- 15 Michaletz, S.T., Cheng, D., Kerkhoff, A.J. & Enquist, B.J. Convergence of terrestrial plant production across global climate gradients. *Nature* **512** 39–43 (2014).

- 16 Wang, H., Prentice, I. C., Keenan, T. F., Davis, T. W., Wright, I. J., Cornwell, W. K., Evans, B. J. & Peng, C. Towards a universal model for carbon dioxide uptake by plants. *Nature Plants* **3** 734–741 (2017).
- 17 Jones C, Robertson E, Arora V, Friedlingstein P, Shevliakova E, Bopp L, Brovkin V, Hajima T, Kato E, Kawamiya M. Twenty-first-century compatible CO<sub>2</sub> emissions and airborne fraction simulated by CMIP5 Earth System models under four representative concentration pathways. *Journal of Climate* **26**(13): 4398-4413, (2013).
- 18 Gorham E. Northern peatlands: Role in the carbon cycle and probable responses to climatic warming. *Ecological Applications* **1** 182–195 (1991).
- 19 Korhola, A., Alm, J., Tolonen, K., Turunen, J. & Jungner, H. Three-dimensional reconstruction of carbon accumulation and CH<sub>4</sub> emission during nine millenia in a raised mire. *Journal of Quaternary Science*, **11**, 161-165 (1996).
- 20 Väliänta, M., Salojärvi, N., Vuorsalo, A., Juutinen, S., Korhola, A., Luoto, M., Tuittila, E.-S. Holocene fen-bog transitions, current status in Finland and future perspectives. *The Holocene* **27**(5): 752-764 (2016).
- 21 Cooper, M. D.A., Estop-Aragonés, C., Fisher, J. P., Thierry, A., Garnett, M. H., Charman, D. J., Murton, J. B., Phoenix, G. K., Treharne, R., Kokelj, S. V., Wolfe, S. A., Lewkowicz, A. G., Williams, M., and Hartley, I. P. Limited contribution of permafrost carbon to methane release from thawing peatlands. *Nature Climate Change*, **7**, 507-511 (2017).
- 22 Jones, M. C., Harden, J., O'Donnell, J., Manies, K., Jorgenson, T., Treat, C. and Ewing, S. Rapid carbon loss and slow recovery following permafrost thaw in boreal peatlands. *Global Change Biology* **23** 1109–1127 (2017).
- 23 Ott, C.A. and Chimner, R.A. Long-term peat accumulation in temperate forested peatlands (*Thuja occidentalis* swamps) in the Great Lakes region of North America. *Mires and Peat* **18** 1–9 (2016).
- 24 Wang, H., Richardson, C. J. and Ho, M. Dual controls on carbon loss during drought in peatlands. *Nature Climate Change* **5** 584-588 (2015).
- 25 Page, S. E., Siegert F., Rieley J.O., Boehm H.D., Jaya A. and Limin S. The amount of carbon released from peat and forest fires in Indonesia during 1997. *Nature* **420** 61–65 (2002).
- 26 Moore, S., Evans, C. D.; Page, S. E.; Garnett, M. H.; Jones, T. G.; Freeman, C.; Hooijer, A., Wiltshire, A. J., Limin, S. H. and Gauci, V. Deep instability of

deforested tropical peatlands revealed by fluvial organic carbon fluxes. *Nature* **493**  
660-663 (2013).

## Methods

*Carbon accumulation estimates.* Mean annual carbon accumulation over the last millennium was estimated for 294 peatland sites (Table SIT1). In line with climate modelling studies, we use the term ‘last millennium’ to refer to the pre-industrial millennium between AD 850-1850). The total carbon accumulated over this period was calculated for all sites in Table SI1 by using a flexible Bayesian approach that incorporated estimates of age and minimum and maximum accumulation rates<sup>12</sup>. A number of sites were previously published (Reference 12 and references therein), but we added over 200 sites to the database from new field coring, as well as additional analysis for bulk density, carbon and radiocarbon dating from a range of existing samples held in laboratories around the world to bring the data to comparable standards. Age models were constructed from at least 2 radiocarbon dates (low resolution sites) or more than 4 radiocarbon dates (high resolution sites) (see Table SI1 for details). For each of these records, bulk density was measured on contiguous samples. Carbon content was calculated based on either elemental carbon measurements or loss-on-ignition, when this was the case, loss-on-ignition was converted to total carbon assuming 50% of organic matter is carbon<sup>27</sup>.

The fen (minerotrophic or high nutrient, including poor fens) and bog (ombrotrophic or low nutrient) classification (Figure 1b) is a simplification and more information relating to each individual record is given in the supporting information (SI) section (Table SIT1). There are 212 bogs versus 82 fens (which include 5 mixed sites).

We analysed the relationship between total carbon accumulation and a wide range of different climate parameters, including seasonal and mean annual temperature, precipitation and moisture balance indices (Figures 1d and SI1). Climate parameters were calculated using the CRU 0.5° gridded climatology for 1961-1990 (CRU CL1.0)<sup>28</sup>.

*Modern day PAR0 and MI calculations.* PeatStash<sup>29</sup> was used to calculate the accumulated PAR0 by summing the daily PAR0 over the growing season (days above freezing) for each peatland grid cell. The daily PAR0 is obtained by integrating the instantaneous PAR between sunrise and sunset. The seasonal accumulated PAR0 depends on latitude and cloudiness, and indirectly on temperature, because temperature determines the length of the growing season, i.e. which days are included in the seasonal accumulated PAR0 calculation. The Moisture

Index (MI) was calculated as  $P/Eq$ , where  $P$  is annual precipitation and  $Eq$  is annually integrated equilibrium evapotranspiration calculated from daily net radiation and temperature<sup>29</sup>.  $P$  and  $Eq$  were also derived from CRU CL1.0.

*Statistical model.* The statistically modelled data are based on a relationship between  $C$  accumulation ( $\text{g C m}^{-2} \text{ yr}^{-1}$ ) and  $PAR0$  ( $\text{mol phot m}^{-2} \text{ yr}^{-1}$ ) ( $R^2 = 0.25$ ,  $F_{2,292} = 49.35$ ,  $p\text{-value} = 2.5 \times 10^{-19}$ ) as follows (Figure SI2, Table SI2):

$$\log_{10} C = 0.3 + 0.0003 \times PAR0 - 1.6 \times 10^{-8} \times PAR0^2 \quad (1)$$

This function is used when deriving a spatially explicit estimate of net carbon uptake using modern-day gridded  $PAR0$  values (Figure 3b). The general trend is for the model to over-estimate the peatland carbon sink at high latitudes and underestimate it at low latitudes, when compared to the spatially interpolated data (Figure 3c). However, this is not uniform and the spatially interpolated data and the statistically derived model results compare well in areas of Eastern Siberia, China, Europe, southern North America, the tropical and Andean regions in South America and certain areas of central Africa. There is less congruence between spatially interpolated and statistically modelled estimates in areas where observations are lacking.

*Spatial interpolation.* To model the variation in spatial data, we use the model-based geostatistical approach described by Diggle and Riberio<sup>30</sup>, which decomposes the variation in a spatially distributed variable as follows:

$$Y(x) = \mu(x) + S(x) + \epsilon \quad (2)$$

where

- $x$  is a spatial location; the coring sites
- $Y$  is the value of the variable of interest; the carbon accumulation rate
- $\mu(x)$  is the mean field component, either as a constant mean or modelled using covariates (i.e.  $\mu(x) = \beta X$ )
- $S(x)$  is the spatially random error, described by two parameters, the range ( $\phi$ ), giving the limit of spatial dependency and variance ( $\sigma^2$ )
- $\epsilon$  is the residual non-spatial random error, described by its variance ( $\tau^2$ )

The spatially random error describes the spatial dependence and can be modelled using one of a set of positive definite spatial covariance functions, which describe the decay in covariance over distance<sup>31</sup>. Prediction for a new location ( $x'$ ) then follows the classic kriging approach of estimating the mean field component ( $\mu(x)$ ) and the deviation ( $S(x)$ ) from this at the new location, based on the covariance of this latter term with nearby locations<sup>32</sup>. The residual non-spatial error ( $\epsilon$ ) is then estimated as the kriging variance, giving estimation error. An alternative to method of estimating interpolation uncertainty is by a sequential simulation approach. Here, the spatially random error is simulated as multiple Gaussian random fields<sup>32</sup>, constrained on the observations, and the range of outcomes provides as estimate of the non-spatial error. All spatial analysis was carried out in R 3.3.2 using the packages 'gstat'<sup>33</sup> and 'raster'<sup>34</sup>.

*Gridding observed accumulation rates.* In a first step, we grid the observed carbon accumulation rates to a 0.5° grid clipped to a peatland mask<sup>4</sup> using ordinary sequential simulation. The mean field ( $\mu(x)$ ) is taken as the mean of the log10 carbon accumulation rates. The spatially random error term ( $S(x)$ ) was modelled from the observations using an exponential covariance function. This was then used to produce 1000 random spatial fields, conditional on both the covariance function and the locations of the observations. These fields were added back to the mean field to produce 1000 simulated carbon accumulation values, with the final values reported as the mean at each grid point. Interpolation uncertainties were estimated as the 95% confidence interval around the mean.

*Gridding accumulation rates using PAR0.* Here, the constant mean field of the previous model was replaced with the model described in equation 1. This provides estimates of estimate variations in the spatial mean field of log10 carbon accumulation rates across the 0.5° peatland grid based on modern PAR0 values (see Table SI2 for statistical significance of the different models). As in the previous step, the spatial random error term was estimated by sequential simulation of the model residuals at the observations sites, producing 1000 random spatial fields of residuals, which were then added back to the interpolated mean field to yield the present time carbon accumulation rate for the grid cell. Final values reported are the mean of the 1000 mean plus residual values at each grid point. The non-spatial error is then given by the 95% confidence interval from the 1000 simulations.



549

550 *Estimating the future carbon sink.* A similar approach was taken for the estimated future  
551 carbon accumulation. The mean field was estimated using equation 1, based on PAR0  
552 projections for two representative concentration pathways RCP2.5 and RCP8.5<sup>35</sup>, using  
553 climate projections for the periods 2040-2060, 2080-2100 and 2180-2200, as well as the  
554 historical period (1990-2005)<sup>36,37</sup>. To avoid bias from the climate model, future estimates of  
555 PAR0 are calculated as the anomaly between future and historical PAR0, added to the  
556 modern observed PAR0 field. The interpolated residuals from the previous step were then  
557 added to these to give estimates of future carbon accumulation rate for each grid cell with  
558 uncertainty estimated as before. It is important to note that while this approach allows the  
559 spatial mean field to change as a function of projected PAR0, the spatially auto-correlated  
560 error term is assumed to remain constant.

561

#### 562 *Data Availability*

563 The data set generated and analysed during the current study are available in the  
564 supplementary information section of this article and from the corresponding authors on  
565 reasonable request.

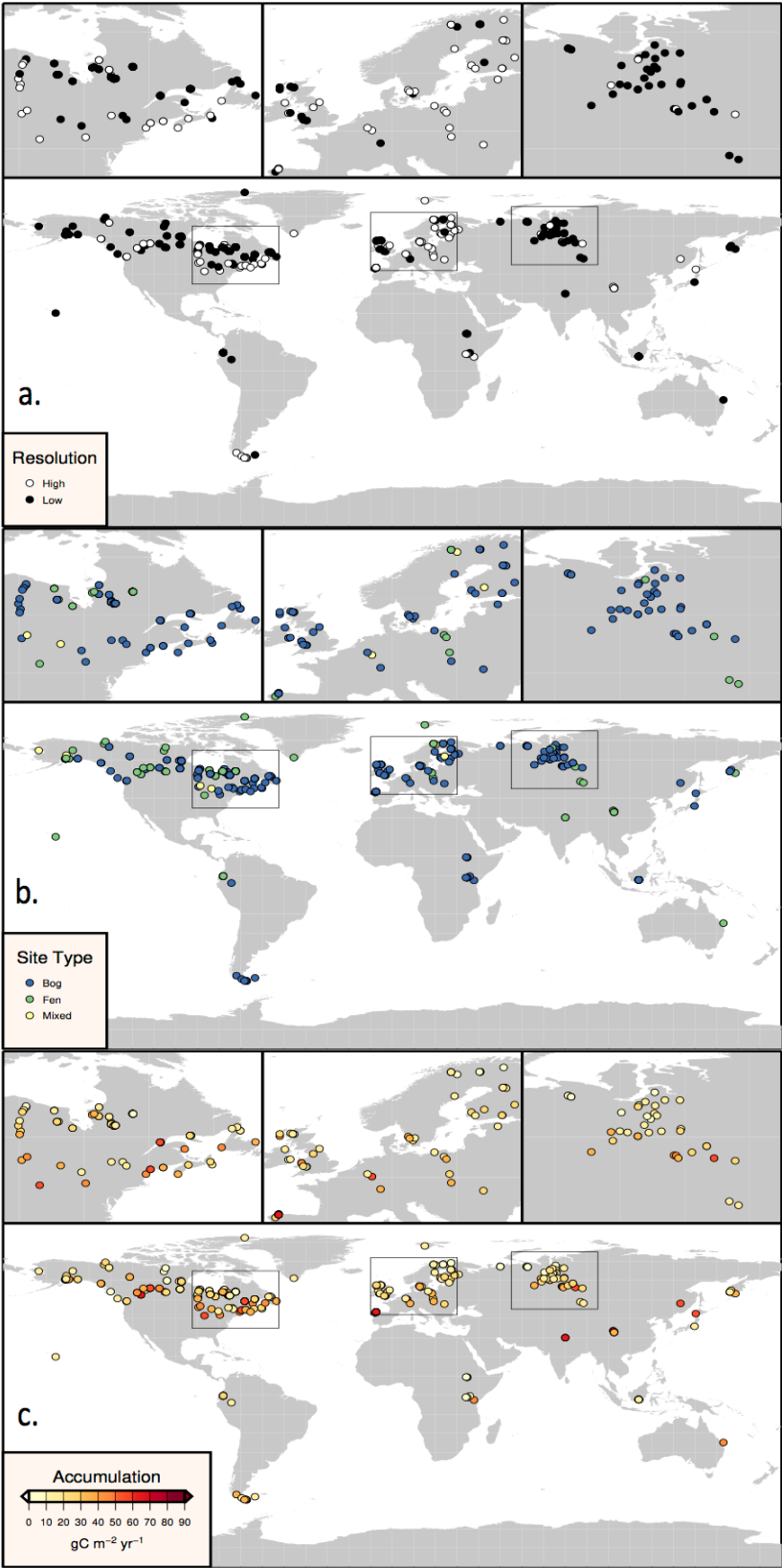
#### 566 *References (Methods Section)*

567

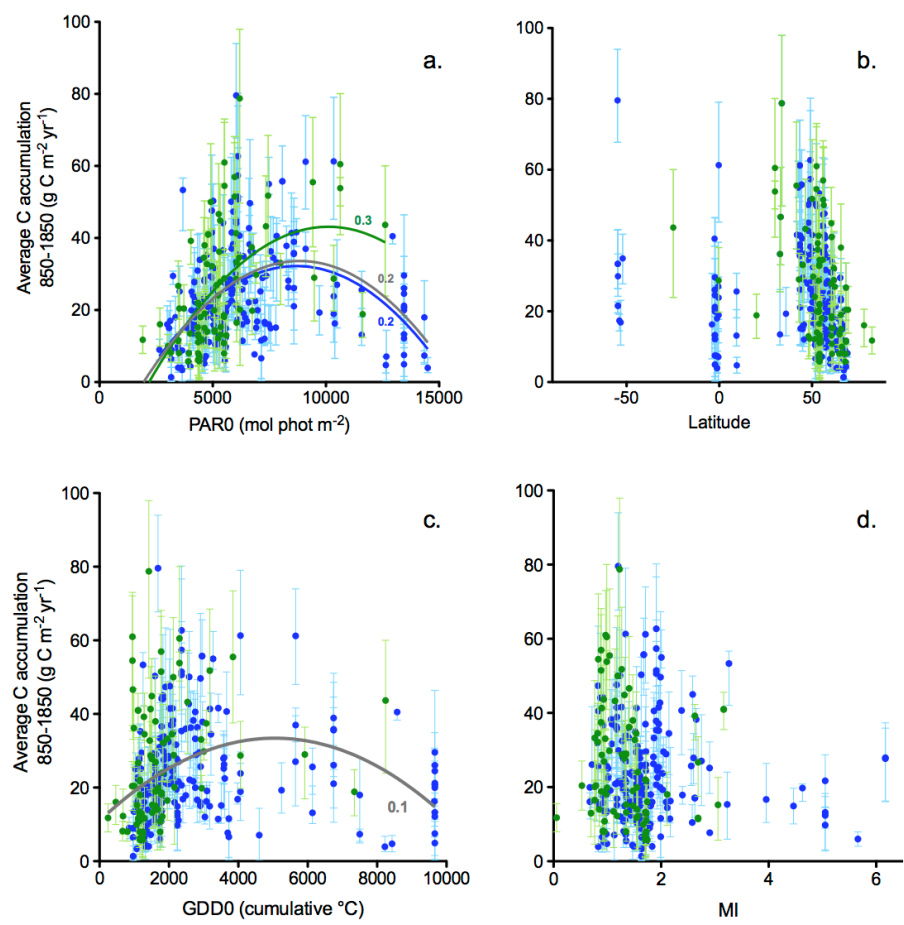
- 568 27 Bol, R. A., Harkness, D. D., Huang, Y. and Howard, D. M. The influence of soil  
569 processes on carbon isotope distribution and turnover in the British Uplands.  
570 *European Journal of Soil Science* **50** 41-51 (1999).
- 571 28 New, M., Hulme, M. and Jones, P.D. Representing twentieth century space- time  
572 climate variability. Part 1: development of a 1961-90 mean monthly terrestrial  
573 climatology. *Journal of Climate* **12** 829-856 (1999).
- 574 29 Gallego-Sala, A. V. and Prentice, I. C. Blanket peat biome endangered by climate  
575 change. *Nature Climate Change* **3** 152–155 (2013).
- 576 30 Diggle, P. and Riberio Jr, P.J. *Model-based geostatistics*. Springer-Verlag, New  
577 York, USA, 232 pp. (2007).
- 578 31 Cressie, N. A. C. *Statistics for spatial data*. New York, John Wiley & Sons Inc.  
579 (1993).
- 580 32 Goovaerts, P. *Geostatistics for natural resources evaluation*. Oxford University  
581 Press, Oxford, UK. 483 pp. (1997).

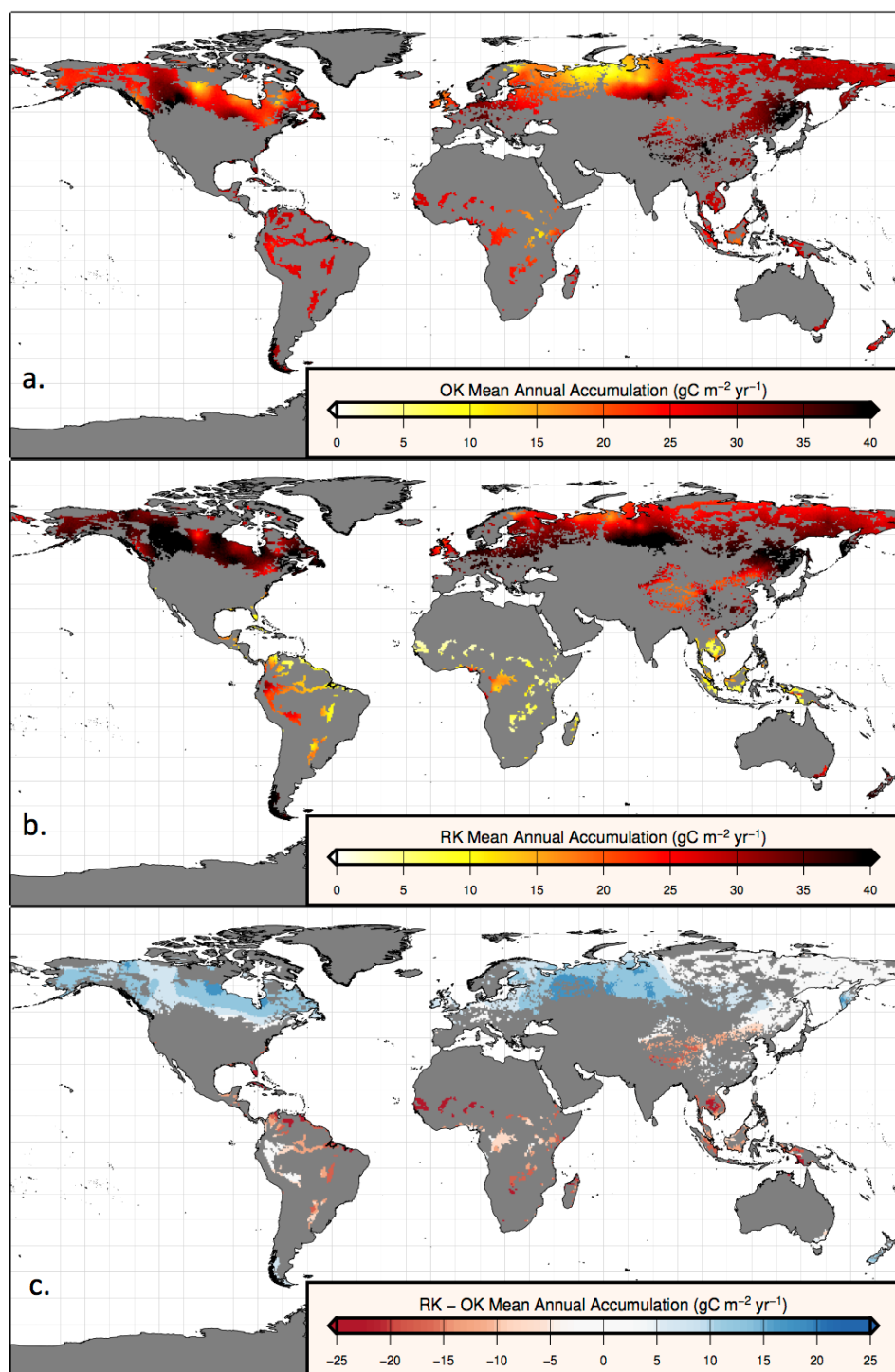
- 33 Pebesma, E.J. Multivariable geostatistics in S: the gstat package. *Computers & Geosciences*, **30**: 683-691 (2004).
- 34 Robert J. H, and van Etten, J. Raster: Geographic analysis and modeling with raster data. R package version 2.5-8. (2016).
- 35 Intergovernmental Panel on Climate Change (IPCC) Fifth Assessment Report 2014. *Climate Change: Synthesis report* (eds. Pachauri R.K. et al.) (2014)
- 36 Jones, C. D., Hughes, J. K., Bellouin, N., Hardiman, S. C., Jones, G. S., Knight, J., Liddicoat, S., O'Connor, F. M., Andres, R. J., Bell, C., Boo, K.-O., Bozzo, A., Butchart, N., Cadule, P., Corbin, K. D., Doutriaux-Boucher, M., Friedlingstein, P., Gornall, J., Gray, L., Halloran, P. R., Hurtt, G., Ingram, W. J., Lamarque, J.-F., Law, R. M., Meinshausen, M., Osprey, S., Palin, E. J., Parsons Chini, L., Raddatz, T., Sanderson, M. G., Sellar, A. A., Schurer, A., Valdes, P., Wood, N., Woodward, S., Yoshioka, M., and Zerroukat, M.: The HadGEM2-ES implementation of CMIP5 centennial simulations, *Geoscientific Model Development* **4** 543-570 (2011).
- 37 Collins, W. J., Bellouin, N., Doutriaux-Boucher, M., Gedney, N., Halloran, P., Hinton, T., Hughes, J., Jones, C. D., Joshi, M., Liddicoat, S., Martin, G., O'Connor, F., Rae, J., Senior, C., Sitch, S., Totterdell, I., Wiltshire, A., and Woodward, S.: Development and evaluation of an Earth-System model – HadGEM2, *Geoscientific Model Development* **4** 1051-1075 (2011).

605 FIGURE 1  
606



607  
608





614 FIGURE 4  
615

